Desalination and Water Treatment
www.deswater.com

doi:10.5004/dwt.2017.21586

94 (2017) 222–230
October

Development of carbon nanotube-mycosorbent for effective Congo red removal: optimization, isotherm and kinetic studies

Ehsan Azin[a], Hamid Moghimi[a,*], Ramezan Ali Taheri[b,*]

[a]*Department of Microbial Biotechnology, School of Biology, College of Science, University of Tehran, Tehran, Iran, Postal code: 1417864411, email: ehsanazin@ut.ac.ir (E. Azin), hmoghimi@ut.ac.ir (H. Moghimi)*
[b]*Nanobiotechnology Research Center, Baqiyatallah University of Medical Sciences, Tehran, Iran, Tel. +982166415495, email: taheri@bmsu.ac.ir (R.A. Taheri)*

Received 27 April 2017; Accepted 22 October 2017

ABSTRACT

Nano-biocomposites with high adsorption surface and various functional groups are considered as efficient sorbents for remediation of azo dyes. In this study, two bio-nanocomposites were made using *Mucor circinelloides*, a previously confirmed potent azo dye biosorbent, with Fe_2O_3 and carbon nanotube. The efficacy of Congo red removal was 67% for the fungal biomass but it was 72% and 85% for the Fe_2O_3-biocomposite and carbon nanotube biocomposites, respectively. The sorption capacity in the free biomass and carbon nanotube biocomposite were 67.1 and 127.2 mg dye/g adsorbent, respectively, showing a 100% increase in sorption capacity of the carbon nanotube biocomposite when compared with the free fungal adsorbent. Also, the SEM images showed precipitation of dye particles on the nano-bioadsorbent surface. The adsorption isotherms showed that the biosorption process is in agreement with the Langmuir isotherm model and the kinetics adsorption results showed that the biosorption process followed the pseudo-second-order kinetics model. Acetone showed the most efficient dye desorption performance which was about 50% for carbon nanotube-biocomposite. In addition, evaluating the removal efficiency of the construct in real wastewater confirmed its high potential for use in wastewater treatment. The values of BOD and COD in treated wastewater decrease for 6259 and 16690 mg/L, respectively.

Keywords: Congo red; Nano-biosorbent; Isotherm; Kinetic; *Mucor circinelloides*

1. Introduction

Azo dyes are considered as the most widely used coloring agents in several industries, including printing, cosmetics, pharmaceuticals, food, tanneries, and textile industries. These molecules have benzidine group in their structure which is known as a carcinogenic agent and it causes genetic mutation in the living organisms [1]. Approximately, 20% of synthetic dyes produced all around the world are consumed by the textile industries of which 10–15% are directly discharged to the wastewater [2]. In textile industries, the average concentration of azo dye in wastewater is about 300 mg/L [3]. Releasing azo dyes into wastewater contaminate the environment and the subsequent incomplete degradation of the dye molecules results in the formation of highly toxic and carcinogenic aromatic amines as the degradation intermediates [4]. Generally, there are different methods of wastewater treatment and they include physical, chemical, and biological methods. The biological methods are more acceptable than the physico-chemical methods, because of their less operational costs and sludge production [5].

Biosorption is one of the biological strategies and is defined as the metabolism independent adsorption of molecules by the surface functional groups present on dead or live biomass [6]. Currently, chitosan is one of the frequently used bio-adsorbent for various pollutants, such as copper, mercury, nickel, lead, cadmium, and azo dyes. The efficiency of chitosan in biosorption process is related

*Corresponding author.

to the presence of amino and hydroxyl functional groups in its structure [7]. With respect to the fact that chitin and chitosan are the key elements of fungal cell wall structure and also because of the high surface to volume ratio in fungal cells, fungi are suitable candidates for biosorption [8]. The use of fungal biomass as an adsorbent is cost-effective, attractive, and environmentally friendly [5,9].

In recent years, the use of nanoparticle adsorbents has been widely investigated for pollutants removal from effluents [10]. Carbon nanotubes and iron nanoparticles are considered as the adsorbents because of their high surface to volume ratio and easy separation from wastewater, respectively [11]. However, applying them alone would not be economical in the industrial scale. To overcome this problem, bio-adsorbents and nano-adsorbents can be used together in a single construct. Zhu et al. [12] prepared chitosan/kaolin/nanosized γ-Fe_2O_3 composites for methyl orange adsorption. Methyl orange (71.0%) was adsorbed within 180 min from 20 mg L^{-1} dye solution by 1.0 g L^{-1} adsorbent. Sui et al. [13] used the biocomposite fiber of calcium alginate/multi-walled carbon nanotubes for the adsorption of methylene blue. The results showed an increase in the adsorption rate for methylene blue as compared to that of the free calcium alginate. Zhou et al. [14] investigated Acid Orange 7 and Acid Orange 10 on ethylenediamine-modified magnetic chitosan nanoparticles (EMCN). The maximum adsorption capacity of the EMCN was 3.47 and 2.25 mmol/g for Acid Orange 7 and Acid Orange 10, respectively. The reported nano-bioconstructs for contaminant removal from wastewater are limited to biological polymers such as chitosan. While the purification process of such polymers is time-consuming and costly, using the whole fungal cells as a polymer containing adsorbent structures is a less studied and cost effective approach. The key aim of this study was to develop a novel adsorbent by combining nanostructures and fungal biomass to achieve a nano-biocomposite, to be used for azo dye removal. Thereafter, the isotherm and kinetics of the Congo red adsorption process by the constructed composite was studied. Moreover, the efficacy of the nano-bioconstruct was evaluated in the real sample of polluted wastewater.

2. Materials and methods

2.1. Chemicals and reagents

Congo red (Merck) was used as the azo dye in all the sorption tests. Iron nanoparticle (US Research Nanomaterials, Inc., 20–30 nm) and carbon nanotube (Neutrino, 30 μm) were used as the nanostructures. All chemicals and reagents used were of analytical grade. All solutions were prepared using deionized water throughout the experiment.

2.2. Microorganism

The strain *Mucor circinelloides* introduced in previous studies as an efficient azo dye biosorbent (unpublished data) was revived on potato dextrose agar (PDA). This strain was deposited in the environmental biotechnology laboratory of University of Tehran.

2.3. Preparation of fungal biomass

For biomass production, the spores were harvested from cultures of fungi on PDA and they were transferred to potato dextrose broth (PDB) flasks. The inoculated flasks were incubated at room temperature (28 ± 1°C) on a rotary shaker at 120 rpm for 3 d. Cells were harvested by centrifugation at 2630 g, washed twice with sterile distilled water, and stored for future tests at 4°C.

2.4. Preparation of different nano-biocomposites

To stabilize nanostructures on biomass, 20 g of biomass was dissolved in 200 ml deionized distilled water and 0.2 g of each nanostructure including magnetite nanoparticles and carbon nanotubes were added to 100 ml deionized water and shaken at 120 rpm. After 20 min, each nano-solution was added to biomass flasks and shaked at 120 rpm for 30 min. Then, the produced nano-biocomposites were separated by centrifugation at 2630 g and nano-biocomposites were washed using deionized distilled water.

2.5. Evaluation of dye removal potential of nano-biocomposites

An equal amount of each nano-biocomposite (0.2 g) was added to 20 ml dye solution containing 1000 mg/L Congo red. In addition, 0.2 g nanoparticle free biomass was added to the flask containing 20 ml dye at 1000 mg/L concentration for comparison with nano-biocomposites. Three replicate experiments were conducted for each sample. All flasks were incubated at 120 rpm and 28°C. After 1 h, the nano-biocomposites were separated by centrifugation at 2630 g and the optical density (OD) of the supernatants was measured at 500 nm using a spectrophotometer (Shimadzu uv-160, Japan). The most efficient nano-biocomposite was selected and used for further experiments.

2.6. Optimization of dye adsorption

The presence of salt at concentrations of 4–10% in the textile industry wastewater has adverse effects on dye adsorption by the adsorbents [15]. Therefore, the effects of four physical and chemical factors including adsorbent volume (0.2–1 g), dye concentration (250–3000 mg/L), temperature (25–75°C), and salt concentration (0–20%) on dye adsorption were examined.

2.7. Adsorption equilibrium

To study the isotherm of adsorption process in the selected adsorbent, 0.2 g of nano-biocomposite was added to 20 ml dye solution containing 500, 1000, 2000, and 3000 mg/L of Congo red. The flasks were shaken at 120 rpm for 1 h. The supernatant absorbance was measured at 500 nm. The biosorption capacity of the biomass q_e (mg/g) was calculated using Eq.(1):

$$q_e = \frac{(C_0 - C_t)}{m} \times V \quad (1)$$

where q_e is the biosorption capacity, C_0 and C_e (mg/L) are dye concentrations in solution at initial and t time, V (L) is the solution volume and m (g) is the wet biomass weight [16].

Isotherm studies were performed to analyze the experimental equilibrium data using the Freundlich and Langmuir isotherm models. The model equations are as follows:

$$\underbrace{\frac{1}{q_e}=\frac{1}{q_m k_l C_e}+\frac{1}{q_m}}_{\text{Langmuir equation}} \qquad \underbrace{\log q_e=\log k_f+\frac{1}{n}\log C_e}_{\text{Freundlich equation}} \tag{2}$$

where q_e is the adsorption capacity of the carbon nanotube nano-biocomposite at equilibrium, q_m is the maximum adsorption, k_f and k_1 are the Freundlich and Langmuir isotherm constants and C_e is the dye concentration at equilibrium time [17,18].

2.8. Adsorption kinetics

To study the adsorption kinetics, that is, determining the rate of adsorption steps, 0.2 g of the selected nano-biocomposite was added to 20 ml Congo red solution at a concentration of 500 mg/L and the flask was shaken at 120 rpm. Samples were acquired at the determined time intervals. The kinetic equations are as follows:

$$\underbrace{ln\left(q_e-q_t\right)=lnq_e-k_l t}_{Pseudo-first\ order} \qquad \underbrace{\frac{t}{q_t}=\frac{1}{k_2 q_e{}^2}+\frac{1}{q_e}(t)}_{Pseudo-second\ order} \tag{3}$$

where q_e and q_t (mg/g) are the amount of dye adsorbed at equilibrium and t time, k_1 and k_2 are the kinetics constants of the pseudo-first order and pseudo-second order models, respectively [19].

2.9. Desorption study

To study the desorption performance of the five adsorbents, 0.2 g of each previously treated adsorbent with 1000 mg/L Congo red solution was added to acetone 50% v/v, 0.1 M HCl, and NaOH solutions and shaken at 120 rpm and maintained at 28°C. After 2 h, the cells were harvested by centrifugation and the absorbance of the supernatant was measured at 500 nm.

2.10. Scanning electron microscopy and zeta potential analysis

In order to investigate the adsorbent surface, scanning electron microscopy [20] (Zeiss, Germany) analysis was performed before and after the adsorption by nano-biocomposite.

To determine the charge of the nanobio-composite surface, zeta potential measurements were performed on the Malvern Zetasizer instrument charge before and after the dye adsorption.

2.11. Evaluation of the construct efficiency in real textile wastewater treatment real

The real wastewater sample was provided from a dyestuff manufacture located in the south of Tehran and stored at 4°C in the laboratory. The value of electrical conductivity (EC), salinity and pH, and total dissolved solids (TDS) concentration were measured using Mettler Toledo SevenMulti. Total hardness (TH) and alkalinity of the wastewater samples were measured using Pars Omid Company kits (Iran). Biological oxygen demand [21], chemical oxygen demand (COD) and total suspended solids (TSS) were evaluated using the standard method [22]. All measurements were conducted before and after the treatment of wastewater samples with carbon nanotube biocomposite. To evaluate the removal efficiency of nano-biocomposite in dye containing real sample, 20 ml of wastewater was treated with a mixture of 0.2 g nano-biocomposite and 0.2 g fungal mycelial pellet at 120 rpm for 1 h. Then, the absorbance of the separated supernatant was measured at 400 to 800 nm.

In order to estimate the number of fungal spores in the wastewater sample, 20 ml of wastewater was autoclaved for 15 min at 121°C, treated with 0.2 g mycelial pellets and incubated for 2 h at 120 rpm. The supernatant was used to calculate the colony forming unit (CFU) of fungi on PDA plates.

3. Results and discussion

3.1. Evaluation of dye removal in different adsorbents

The percentage of Congo red removal using free fungal biomass, magnetic nanoparticles, magnetite biocomposite, carbon nanotubes, and carbon nanotube biocomposite is as shown in Fig. 1. When carbon nanotubes are used as adsorbents, there are several benefits from several structural advantages such as the high tendency for noncovalent interactions like hydrogen bonding, π-π stacking, electrostatic forces, van der Waals forces, and hydrophobic interactions with organic molecules and also the possibility to alter their functional groups, the volume of micropores, and mesopores and the pores diameter. In addition, the carbon nanotubes' capability for adsorbing the aromatic compound can be moderated through oxidation. All these features can help scientists to improve the use of carbon nanotubes for the remedia-

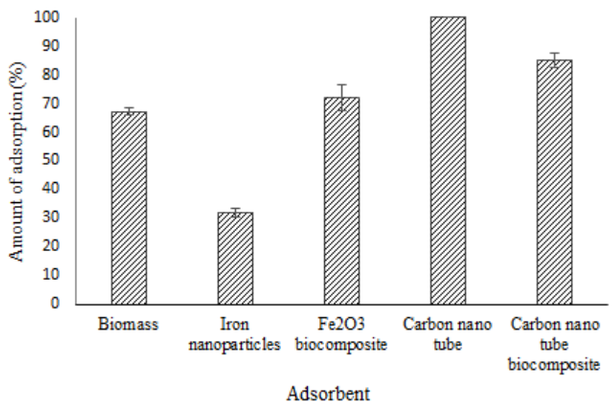

Fig. 1. Adsorption percentage of different adsorbents in Congo red solution of 1000 mg/L.

tion of wastewaters [23]. Because carbon nanotubes presented the highest dye removal ability, does not make it cost effective to use them in large scale [24]. The lower surface area to volume ratio of microorganisms than carbon nanotubes makes their adsorption capacity fall lower than that of the carbon nanotubes. However, fungi benefit from higher surface area to volume ratio among microorganisms. Also, the possible explanation for the high adsorption capacity of fungi is the presence of chitin, a major structural polysaccharide in fungal cell wall composition with two important functional groups, hydroxyl and amine, which may interact with the existing elements of the wastewater. Therefore, further experiments were conducted using carbon nanotube-biocomposite which showed the highest adsorption percentage of Congo red after carbon nanotubes.

When compared with other previously reported biosorbents, *M. circinelloides* with the capability to remove 67.1 mg Congo red per gram of biomass can be considered as an efficient biosorbent. Some other fungal strains have significant sorption capacity such as 149.25, 334.83, and 101.1 mg/g for *Trametes pubescens*, *Penicillium janthinellum,* and *Rhizopus oryzae*, respectively. However, others have weak performance such as *Aspergillus niger* and waste red mud with 14.16 and 4.05 mg/g dye biosorption (Table 1). Table 1 shows the fungal biosorbents' benefit from considerable adsorption capacity which can possibly be attributed to the presence of various polymers in their cell wall composition, including chitin and chitosan. Our results showed that the sorption capacity increased from 67.1 to 131.58 mg/g when the sorbent was switched from fungal biomass to carbon nanotube biocomposite.

3.2. Optimization of dye adsorption

The study of the effect of physicochemical factors showed that the highest adsorption was obtained when the amount of biomass was 1 g and the salt concentration was 5%. The presence of salt increased dye adsorption by carbon nanotube nano-biocomposites. When considering the presence of salt in textile industry wastewater, salt can be considered as a contributing factor in the dye adsorption process. The concentration of salt in textile industry wastewater is in the range of 4 to 10% and it interferes with the dye adsorption process [15]. Here, 40% of the dye was removed in the absence of salt and 95% at the concentrations of 5, 10 and 20% of NaCl. This enhancement can be attributed to the stability of the physiological activities of fungal mycelium in the presence of salt. Moreover, the presence of salt decreases the thickness of the fungal membrane bilayer which can improve dye biosorption using fungal mycelium. Similar results were found by Wang et al. [2] who observed that increasing Congo red

Table 1
Comparison of adsorption capacity, isotherm and kinetic of different chemical and biological nano-sorbents

Adsorbent		Adsorption capacity (mg/g)	Isotherm	Kinetic	Reference
Bioadsorbents	*Aspergillus niger*	14.16	Radke–Prausnitz	First order and pseudo second order	[25]
	Trametes pubescens	149.25	Freundlich	Pseudo-second-order	[26]
	Penicillium janthinellum	344.83	Langmuir	Pseudo-second-order	[2]
	Rhizopus oryzae	101.1	Redlich–Peterson	Pseudo-second-order	[27]
	Chitosan hydrobeads	–	Langmuir	Pseudo second-order	[28]
Chemo-sorbent	Crgano-attapulgite	189.39	Langmuir	Pseudo-second-order	[29]
	Waste red mud	4.05	Langmuir and Freundlich	–	[30]
Nano-adsorbents	Magnetic Fe_3O_4-graphene nanocomposite	33.66	Langmuir and Freundlich	Second-order kinetic	[31]
	Maghemite nanoparticles (γ-Fe_2O_3)	208.33	Langmuir	–	[32]
	graphene/polyaniline/ cuprous oxide composite hydrogel	97.91	–	–	[33]
	Zinc oxide	334	Langmuir	Pseudo-second-order	[34]
	Ni/Mg/Al layered double hydroxides	1250	Langmuir	Pseudo-second-order	[35]
	NiO–Al_2O_3	357	Langmuir	Pseudo-second-order	[36]
Bio-Nanocomposites	Xanthan gum/silica hybrid nanocomposite	209.205	Langmuir	Pseudo-second-order	[37]
	Chitosan/Montmorilloe nanocomposite	54.52	Langmuir	Pseudo-second-order	[38]
	Nano- mycocomposite	127.2	Langmuir	Pseudo-second-order	This study

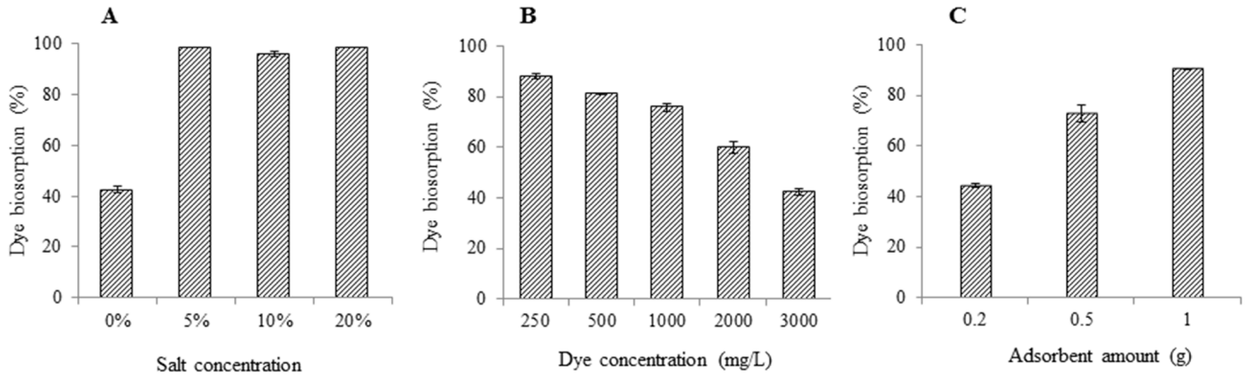

Fig. 2. The effect of salt concentration (in dye concetration of 3000 mg/L and 0.2 g biomass), dye concentration (0.2 g biomass), temperature (in dye concetration of 3000 mg/L and 0.2 g biomass) and adsorbent amount (in dye concetration of 3000 mg/L) in the efficiency of Congo red adsorption by *M. circinelloides.*

biosorption using *P. janthinellum* increased the salt concentration.

In addition, increasing biomass amount resulted in the enhancement of dye adsorption percentage. Sivasamy et al. [16] reported that by increasing biomass of *A. niger* and *Trichoderma* sp., the rate of dye removal was also increased. In the case of dye concentration, the more the dye concentration, the less removal percentage by nano-mycosorbent. A possible explanation for this reduction is that the binding sites on the nano-mycosorbent would have been filled at almost 500 mg/L dye concentration and 10 g/L adsorbent concentration and dye cannot be attached to the nano-biocomposite anymore.

The investigated results of the temperature effect on biosorption showed that increasing the concentration to 50°C would increase the dye adsorption by the adsorbent. The reason for this is probably the increased mobility of the molecules and the reaction between them and the adsorbent.

3.3. Adsorption equilibrium

Evaluating the maximum capacity of adsorption and the adsorption isotherm model showed that the adsorption process followed Langmuir adsorption equation with regression coefficient of 0.9562. This showed that the adsorption process was performed using the monolayer form and the adsorption sites are not infinite on the adsorbent. The maximum adsorption capacity of the adsorbent was calculated as 131.58 mg/g. The results of models linearity tests for Congo red adsorption on carbon nanotube nano-biocomposite are as shown in Fig. 3.

As shown in Fig. 3, q_m was 131.58 mg/g. Since $1/n$ (heterogeneity factor) is $0 < 1/n < 1$, it can be concluded that adsorption is favorable. Furthermore, there are many sites on nano-biocomposite surface. Different studies have shown that adsorption of various adsorbents follow different models [39,40].

According to Table 1, each adsorbent follows a specific isotherm model for each adsorbate and it is not possible to attribute an isotherm model of an adsorbent to the other one, whether it is the same type or not, that is, biological, chemical, nano-based or combination of them.

3.4. Adsorption kinetics

In kinetics experiments, sampling was done at different time intervals. Pseudo-first order and pseudo-second order models were studied for dye adsorption process and their correlation coefficients (r^2) were compared. As shown in Fig. 4, the correlation coefficient of pseudo-second order model was found to be greater than that of the pseudo-first order model, suggesting the fitness of pseudo-second order kinetics model to the obtained data. A second order reaction depends on the concentrations of one second order reactant (dye concentration or adsornent dosage), or two first order reactants.

3.5. Desorption study

Investigating the effect of three different solvent on desorption of Congo red indicated that acetone 50% had the most effect on dye desorption (Fig. 5). Acetone has shown dye desorption of about 60% and 50% for free biomass and nano-biocomposite, respectively. It can be a suitable solvent for reusing adsorbent materials.

3.6. Scanning electron microscopy and zeta potential analysis

The SEM images showed that nanostructures were fixed on fungal mycelial pellets and dye removal mechanism was adsorption (Fig. 6). The images showed the precipitation of dye particles on the nano-bioadsorbent surface.

The zeta potential analysis showed that the surface net charges of fungal biomass are –12.7 and 15.9 mV before and after adsorption, respectively. The results showed that dye adsorption process caused the surface net charge of the adsorbent to become more negative which was due to the presence of sulfonic acid groups in the structure of Congo red.

3.7. Evaluation of the construct efficiency in textile wastewater treatment

Releasing the polluted industrial effluent into the environment leads to environmental aesthetic, preventing

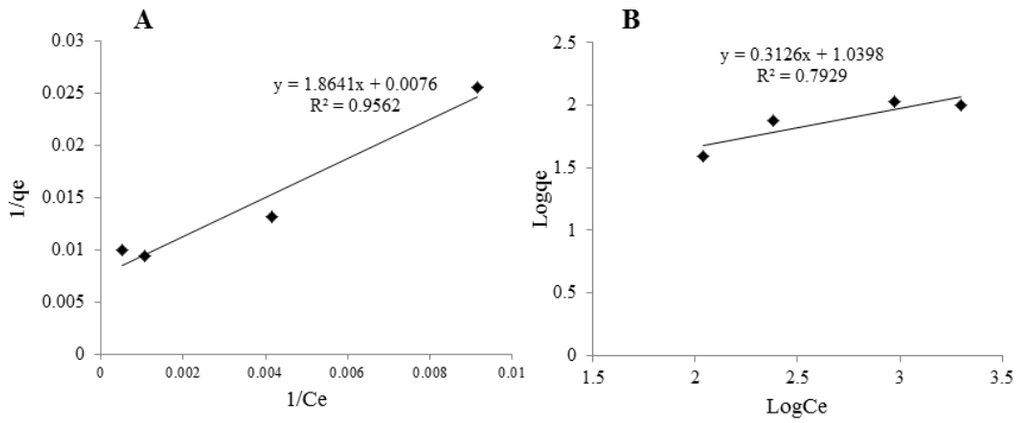

Isotherm	Langmuir				Freundlich		
Parameter	R^2	q_m (mg/g)	K_L (L/mg)	R_L	R^2	K_f (L/mg)	1/n
volume	0.9562	131.58	0.004	0.004	0.7929	10.96	0.3126

Fig. 3. Adsorption isotherm models of Congo red (500, 1000, 2000 and 3000 mg/L) on *M. circinelloides:* A) Langmuir isotherm and B) Freundlich isotherm.

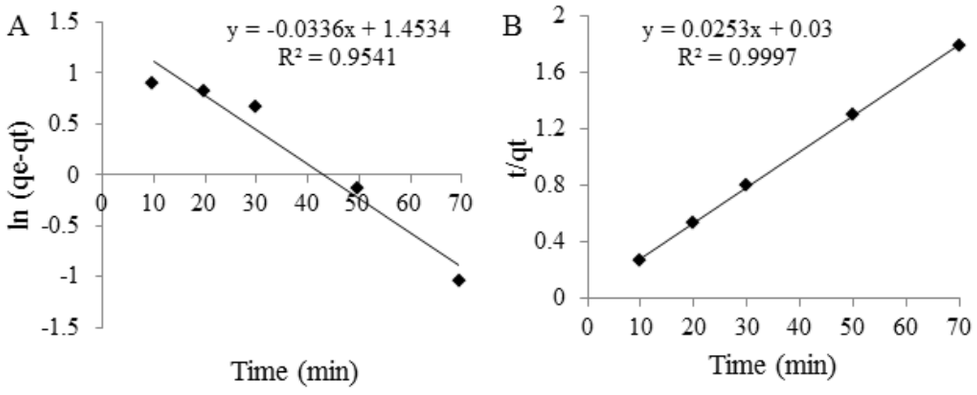

C

Adsorption kinetic parameters	K_1 (g/mg min)	q_e (mg/g)	r^2
pseudo-first order model	0.0336	4.28	0.9541
	K_2 (g/mg min)	q_e (mg/g)	r^2
pseudo-second order model	1.92	39.52	0.9997

Fig. 4. Parameters of kinetics models in Congo red adsorption by nano-biocomposite containing carbon nanotubes and *M. circinelloides* biomass: A) Pseudo-first order model and B) Pseudo-second order model.

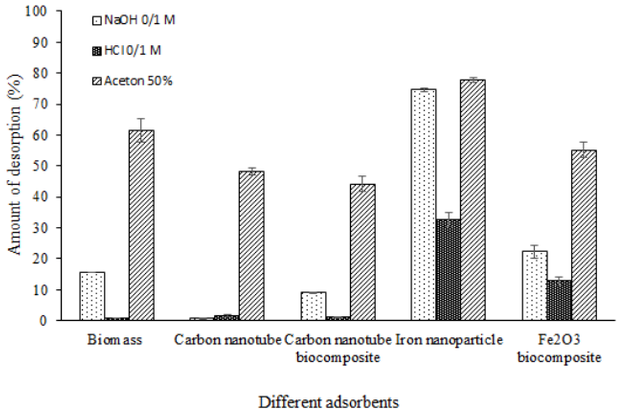

Fig. 5. Comparison of adsorbents dye desorption by acetone 50%, HCl 0.1 M and NaOH 0.1 M.

photosynthesis in aquatic environments, reducing oxygen of water and generally disrupts the food chain of aquatic environments [41]. On the other hand, textile manufacturers must treat their wastewater before releasing it into the environment, thus highlighting the importance of applying efficient adsorbents for dye mixture removal. The value of TDS, TSS, BOD, COD, TH, pH, salinity, EC, and alkalinity before and after treatment is shown in Table 2. Centrifugation of the treated wastewater sample prior to analytical experiments eliminated the suspended solids in the supernatant and therefore caused the TSS value to be zero. 5×10^2 CFU per ml of wastewater was calculated after 24 h incubation of PDA plates and this should be removed in further steps of wastewater treatment.

Visible spectrum after dye mycosorption and nano-biocomposite adsorption demonstrated that nanobiocomposites are capable of removing a significant portion of dyes in a mixture effluent of textile wastewater (Fig. 7).

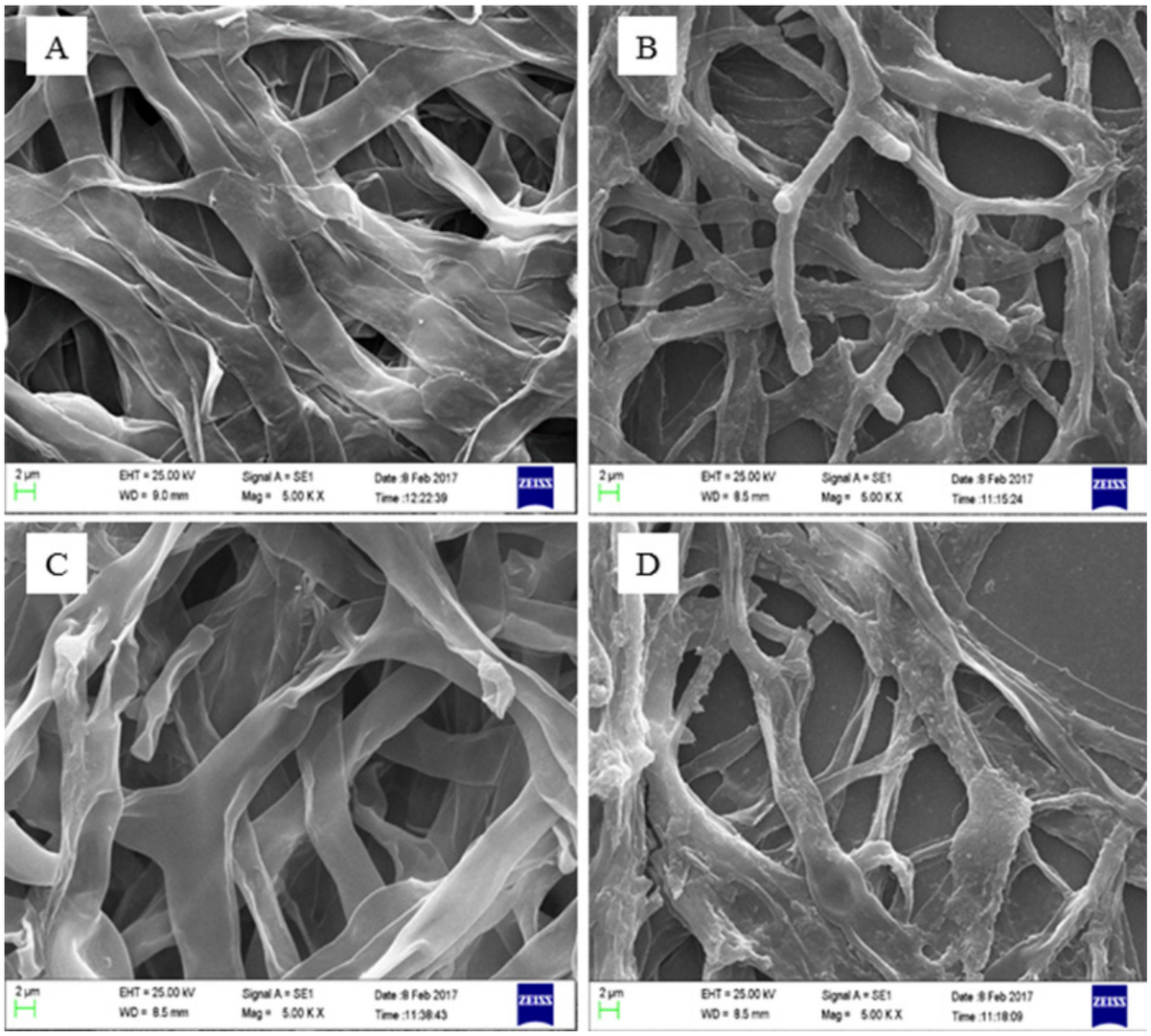

Fig. 6. Scanning electron microscopy images of fungal mycelial pellet: A) before and B) after Congo red adsorption and C) before and D) after dye adsorption by carbon nanotube-biocomposite.

Table 2
Value of wastewater quality parameters before and after treatment

	Untreated wastewater	Treated wastewater
pH	8.5	7.6
BOD (mg/L)	8188	1929
COD (mg/L)	21835	5145
TDS (mg/L)	1612	1554
TSS (mg/L)	895	0
TH (ppm)	350	350
Salinity (ppt)	1.83	1.76
EC (ns/cm)	3.22	3.1
Alkalinity (ppm)	30	10

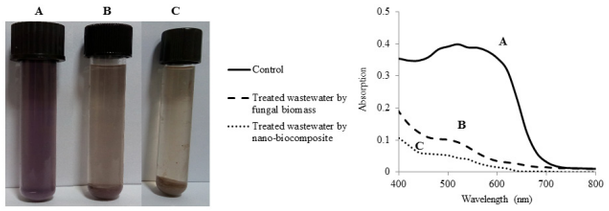

Fig. 7. Untreated (A) and treated (B and C) textile wastewater by *M. circinelloides* mycelial pellets and carbon nanotube biocomposite. Visible spectrum of actual wastewater was shown before and after treatment by fungal mycelial pellets and nano-biocomposite.

4. Conclusions

In the present study, the biological and nano-based strategies were combined to create a single adsorbent for Congo red remediation from effluents. The constructed fungus-nanocomposite can remove 85% of Congo red which is 18% more than that of free fungal adsorbent under the same condition. The adsorption isotherms and kinetics studies showed that the biosorption process is in good agreement with the Langmuir isotherm and pseudo-second-order kinetics models, respectively. The composite exhibited a satisfactory desorption performance. The obtained data can be a prerequisite for further investigations to develop a suitable and cost effective adsorbent for wastewater treatment.

Symbols

q_e — Biosorption capacity (mg/g)
C_0 — Dye concentration in solution at initial time (mg/g)
C_e — Dye concentration in solution at equilibrium time (mg/g)
k_1 — The kinetics constants of pseudo-first order model
k_2 — The kinetics constants of pseudo-second order model
k_f — Freundlich isotherm constant
k_l — Langmuir isotherm constant
m — Wet biomass weight (g)
q_m — Maximum adsorption (mg/g)
q_t — Amount of dye adsorbed at t time
TDS — Total dissolved solids
TSS — Total suspended solids
BOD — Biochemical oxygen demand
COD — Chemical oxygen demand
TH — Total Hardness
V — Solution volume (L)

References

[1] I.D. Mall, V.C. Srivastava, N.K. Agarwal, I.M. Mishra, Removal of congo red from aqueous solution by bagasse fly ash and activated carbon: kinetic study and equilibrium isotherm analyses, Chemosphere, 61 (2005) 492–501.
[2] M.-X. Wang, Q.-L. Zhang, S.-J. Yao, A novel biosorbent formed of marine-derived *Penicillium janthinellum* mycelial pellets for removing dyes from dye-containing wastewater, Chem. Eng. J., 259 (2015) 837–844.
[3] A. Gomes, R. Brás, M. Ferra, M. Amorim, R. Porter, Biological treatment of effluent containing textile dyes, Color. Technol., 116 (2000) 393–397.
[4] R. Sanghi, A. Dixit, P. Verma, Evaluation of *Coriolus versicolor* for its tolerance towards toxic sulphonic azo dyes in sequential batch mode, Process. Saf. Environ. Prot., 89 (2011) 15–21.
[5] A. Porri, R. Baroncelli, L. Guglielminetti, S. Sarrocco, L. Guazzelli, M. Forti, G. Catelani, G. Valentini, A. Bazzichi, M. Franceschi, *Fusarium oxysporum* degradation and detoxification of a new textile-glycoconjugate azo dye (GAD), Fungal. Biol., 115 (2011) 30–37.
[6] S.N. Singh, Microbial Degradation of Synthetic Dyes in Wastewaters, Springer, 2014.
[7] Y. Li, J. Sun, Q. Du, L. Zhang, X. Yang, S. Wu, Y. Xia, Z. Wang, L. Xia, A. Cao, Mechanical and dye adsorption properties of graphene oxide/chitosan composite fibers prepared by wet spinning, Carbohydr. Polym., 102 (2014) 755–761.
[8] P. Kotrba, Microbial biosorption of metals—General Introduction, in: Microbial biosorption of metals, Springer, 2011, pp. 1–6.
[9] V. Ranjusha, R. Pundir, K. Kumar, M. Dastidar, T. Sreekrishnan, Biosorption of Remazol Black B dye (Azo dye) by the growing *Aspergillus flavus*, J. Environ. Sci .Health. A., 45 (2010) 1256–1263.
[10] A. Dalvand, R. Nabizadeh, M.R. Ganjali, M. Khoobi, S. Nazmara, A.H. Mahvi, Modeling of reactive blue 19 azo dye removal from colored textile wastewater using l-arginine-functionalized Fe_3O_4 nanoparticles: optimization, reusability, kinetic and equilibrium studies, J. Magn. Magn. Mater., 404 (2016) 179–189.
[11] H. Gao, S. Zhao, X. Cheng, X. Wang, L. Zheng, Removal of anionic azo dyes from aqueous solution using magnetic polymer multi-wall carbon nanotube nanocomposite as adsorbent, Chem. Eng. J., 223 (2013) 84–90.
[12] H.-Y. Zhu, R. Jiang, L. Xiao, Adsorption of an anionic azo dye by chitosan/kaolin/γ-Fe_2O_3 composites, Appl. Clay. Sci., 48 (2010) 522–526.
[13] K. Sui, Y. Li, R. Liu, Y. Zhang, X. Zhao, H. Liang, Y. Xia, Biocomposite fiber of calcium alginate/multi-walled carbon nanotubes with enhanced adsorption properties for ionic dyes, Carbohydr. Polym., 90 (2012) 399–406.
[14] L. Zhou, J. Jin, Z. Liu, X. Liang, C. Shang, Adsorption of acid dyes from aqueous solutions by the ethylenediamine-modified magnetic chitosan nanoparticles, J. Hazard. Mater., 185 (2011) 1045–1052.
[15] Z. Carmen, S. Daniela, Textile organic dyes–characteristics, polluting effects and separation/elimination procedures from industrial effluents–a critical overview, in: Organic Pollutants Ten Years After the Stockholm Convention-Environmental and Analytical Update, InTech: Croatia, 2012, pp. 55–81.

[16] A. Sivasamy, N. Sundarabal, Biosorption of an azo dye by *Aspergillus niger* and *Trichoderma* sp. fungal biomasses, Curr. Microbiol., 62 (2011) 351–357.
[17] I. Lanowix, The adsorption of gases on plane surface of glass, mica and platinum, J. Am. chem. soc, 30 (1918) 1361.
[18] H. Freundlich, Uber die adsorption in losungen [Adsorption in solution]" Zeitschrift für Physikalische Chemie, 57 (1906).
[19] R. Patel, S. Suresh, Kinetic and equilibrium studies on the biosorption of reactive black 5 dye by *Aspergillus foetidus*, Bioresour. Technol., 99 (2008) 51–58.
[20] W.G. Kreyling, M. Semmler-Behnke, Q. Chaudhry, A complementary definition of nanomaterial, Nano today, 5 (2010) 165–168.
[21] Y. Chen, D. Li, W. Lu, J. Xing, B. Hui, Y. Han, Screening and characterization of astaxanthin-hyperproducing mutants of *Haematococcus pluvialis*, Biotechnol. Lett., 25 (2003) 527–529.
[22] W.E. Federation, A.P.H. Association, Standard methods for the examination of water and wastewater, American Public Health Association (APHA): Washington, DC, USA, (2005).
[23] F.M. Machado, S.B. Fagan, I.Z. da Silva, M.J. de Andrade, Carbon Nanoadsorbents, in: Carbon Nanomaterials as Adsorbents for Environmental and Biological Applications, Springer, 2015, pp. 11–32.
[24] A.B. Dalton, S. Collins, J. Razal, E. Munoz, V.H. Ebron, B.G. Kim, J.N. Coleman, J.P. Ferraris, R.H. Baughman, Continuous carbon nanotube composite fibers: properties, potential applications, and problems, J. Mater. Chem., 14 (2004) 1–3.
[25] Y. Fu, T. Viraraghavan, Removal of Congo Red from an aqueous solution by fungus *Aspergillus niger*, Adv. Environ. Res., 7 (2002) 239–247.
[26] J. Si, T.-Q. Yuan, B.-K. Cui, Exploring strategies for adsorption of azo dye Congo Red using free and immobilized biomasses of Trametes pubescens, Ann. microbiol., 65 (2015) 411–421.
[27] M. Bagchi, L. Ray, Adsorption behavior of Reactive Blue 4, a tri-azine dye on dry cells of *Rhizopus oryzae* in a batch system, Chem. Spec. Bioavailab., 27 (2015) 112–120.
[28] S. Chatterjee, S. Chatterjee, B.P. Chatterjee, A.K. Guha, Adsorptive removal of congo red, a carcinogenic textile dye by chitosan hydrobeads: Binding mechanism, equilibrium and kinetics, Collid. Surf. A. Physicochem. Eng. Asp., 299 (2007) 146–152.
[29] H. Chen, J. Zhao, Adsorption study for removal of Congo red anionic dye using organo-attapulgite, Adsorption, 15 (2009) 381–389.
[30] C. Namasivayam, D. Arasi, Removal of congo red from wastewater by adsorption onto waste red mud, Chemosphere, 34 (1997) 401–417.
[31] Y. Yao, S. Miao, S. Liu, L.P. Ma, H. Sun, S. Wang, Synthesis, characterization, and adsorption properties of magnetic Fe_3O_4@ graphene nanocomposite, Chem. Eng. J., 184 (2012) 326–332.
[32] A. Afkhami, R. Moosavi, Adsorptive removal of Congo red, a carcinogenic textile dye, from aqueous solutions by maghemite nanoparticles, J. Hazard. Mater., 174 (2010) 398–403.
[33] J. Miao, A. Xie, S. Li, F. Huang, J. Cao, Y. Shen, A novel reducing graphene/polyaniline/cuprous oxide composite hydrogel with unexpected photocatalytic activity for the degradation of Congo red, Appl. Surf. Sci., 360 (2016) 594–600.
[34] C. Lei, M. Pi, C. Jiang, B. Cheng, J. Yu, Synthesis of hierarchical porous zinc oxide (ZnO) microspheres with highly efficient adsorption of Congo red, J. Colloid. Interface. Sci, 490 (2017) 242–251.
[35] C. Lei, X. Zhu, B. Zhu, C. Jiang, Y. Le, J. Yu, Superb adsorption capacity of hierarchical calcined Ni/Mg/Al layered double hydroxides for Congo red and Cr (VI) ions, J. Hazard. Mater., 321 (2017) 801–811.
[36] C. Lei, X. Zhu, Y. Le, B. Zhu, J. Yu, W. Ho, Hierarchically porous $NiO–Al_2O_3$ nanocomposite with enhanced Congo red adsorption in water, RSC Adv., 6 (2016) 10272–10279.
[37] S. Ghorai, A.K. Sarkar, A.B. Panda, S. Pal, Effective removal of Congo red dye from aqueous solution using modified xanthan gum/silica hybrid nanocomposite as adsorbent, Bioresour. Technol., 144 (2013) 485–491.
[38] L. Wang, A. Wang, Adsorption characteristics of Congo Red onto the chitosan/montmorillonite nanocomposite, J. Hazard. Mater., 147 (2007) 979–985.
[39] Y. Yang, G. Wang, B. Wang, Z. Li, X. Jia, Q. Zhou, Y. Zhao, Biosorption of Acid Black 172 and Congo Red from aqueous solution by nonviable *Penicillium* YW 01: Kinetic study, equilibrium isotherm and artificial neural network modeling, Bioresour. Technol., 102 (2011) 828–834.
[40] Z. Aksu, E. Balibek, Effect of salinity on metal-complex dye biosorption by *Rhizopus arrhizus*, J. Environ. Manage., 91 (2010) 1546–1555.
[41] H.S. Lade, T.R. Waghmode, A.A. Kadam, S.P. Govindwar, Enhanced biodegradation and detoxification of disperse azo dye Rubine GFL and textile industry effluent by defined fungal-bacterial consortium, Int. Biodeter. Biodegr., 72 (2012) 94–107.